Scanning Microscopy Vol. 11, 1997 (Pages 171-177) 0891-7035/97$5.00+.25
Scanning Microscopy International, Chicago (AMF O'Hare), IL 60666 USA

# RADON TRANSFORM TECHNIQUES FOR ALIGNMENT AND THREE-DIMENSIONAL RECONSTRUCTION FROM RANDOM PROJECTIONS

Michael Radermacher*

Wadsworth Center, New York State Department of Health and
Department of Biomedical Sciences, State University of New York, Albany, NY

## Abstract

Since their inception, three-dimensional reconstruction techniques have been based on the theory of Radon transforms. Only much later were Radon transforms recognized as powerful tools for image processing and pattern recognition. Techniques like the common lines technique for finding the orientation of projections of highly symmetrical particles can easily be translated into a technique that uses Radon transforms. Radon transforms have the advantage of being real valued which simplifies many interpolation steps. Correlation techniques have been developed for alignment of a single noisy projection relative to a three-dimensional model and many ideas originally set forward in previous work by the author have been realized. These include simultaneous rotational-translational alignments, iterative refinements of three-dimensional reconstructions and a Two-step Radon Inversion Procedure (TRIP).

**Key Words**: Radon transform, image processing, alignment, three-dimensional reconstruction, electron microscopy.

*Address for correspondence:
M. Radermacher
Max-Planck Institute for Biophysics
Departmen of Structural Biology
Heinrich-Hoffmann-Straße 7
D-60528 Frankfurt/M, Germany
Telephone number: +49-69-9676 9352
FAX number +49-49-9676 9359
E-mail: michael@biophys.mpg.de

## Introduction

For a three-dimensional reconstruction from projections the orientation of the projections in relation to a common coordinate system must be known. In tomographic reconstructions of single objects - e.g., centrosomes in thick sections or individual macromolecules - from single-axis or conical tilt series, the orientation of the projections is known from the microscope's goniometer reading. Here, the main alignment problem is a translational alignment relative to a common origin [7]. In a reconstruction from projections of multiple copies of the same macromolecule, the orientation cannot be determined solely from the goniometer reading. The method of reconstruction from a random conical tilt series [13, 15] still takes advantage of the fact that most macromolecules attach to the carbon support of the specimen in a preferred orientation, which again relates one angle to the goniometer tilt. The second angle here can be found through rotational alignment techniques applied to a $0^\circ$ image of the specimen. If a tilt series is not available and the molecule does not exhibit preferred orientation, then the orientation of a particle in any given projection must be found by information contained in the image. The common lines method developed by Crowther *et al*. [3] solved this problem for particles with a high degree of symmetry. For icosahedral symmetry the Fourier transform of one projection intersects with up to 59 symmetry-related projections. The pattern of common lines can be found in one projection as each projection also represents all symmetry related images. This pattern determines the orientation of the projection. Projections of asymmetrical particles do not contain common lines within one image. However, the Fourier transforms of any two projections of the same object share at least one line, which lies along the direction of the common tilt axis. If three non-colinear common lines among three projections can be found, then these three lines determine uniquely - aside from a mirror operation - the orientation of these three projections in space [5, 6, 18].

Whereas the original method for finding common lines had been developed using Fourier techniques, there are advantages in replacing some of the analysis by

operations on Radon transforms [12, 16].

## Theory

The three-dimensional Radon transform is defined as

$$\hat{f}\left(p,\vec{\xi}\right)=\int f\left(\vec{r}\right)\delta\left(p-\vec{\xi}\bullet\vec{r}\right)d\vec{r} \qquad (1)$$

where $\delta(p-\xi \cdot r)$ specifies a plane over which the integration is carried out and $\xi$ is the unit vector that determines the direction of this plane. For the two-dimensional Radon transform, $\xi$ and r are replaced by two-dimensional vectors and the integration becomes a line integration instead of an integration over planes.

Radon transforms and Fourier transforms are closely related. The two- or three-dimensional Fourier transform can be calculated from the two- or three-dimensional Radon transform by a one-dimensional radial Fourier transform

$$\hat{f}\left(p,\vec{\xi}\right)=\int F\left(s\vec{\xi}\right)e^{2\pi sp}\,ds \qquad (2)$$

with $F(s\xi)$ being the two- or three-dimensional Fourier transform of f(r) in polar coordinates. The *projection theorem* known from Fourier theory is also valid for Radon transforms [4].

A further theorem is the *shifting property* of Radon transforms. If f(r-a) is the function f shifted by a, then its Radon transform is

$$\begin{aligned}&\int f\left(\vec{r}-\vec{a}\right)\delta\left(p-\vec{\xi}\bullet\vec{a}\right)d\vec{r}=\\&=\int f\left(\vec{q}\right)\delta\left(p-\vec{\xi}\bullet\vec{a}-\vec{\xi}\bullet\vec{q}\right)d\vec{q}=\hat{f}\left(p-\vec{\xi}\bullet\vec{a},\vec{\xi}\right)\end{aligned} \qquad (3)$$

Many convolutions that have kernels of two or three dimensions when applied to a real space object become one-dimensional kernels when applied to Radon transforms.

### Alignment

The rotational and translational alignment between two images can be found from the cross-correlation of their Radon transforms. Let $\hat{f}(p,\xi)$, with $\xi = (\cos(\varepsilon), \sin(\varepsilon))$, be the the Radon transform of a reference image and let $\hat{g}(p,\xi)$ be the Radon transform of the image that is to be aligned with respect to $\hat{f}$. Let $\hat{g}$ be rotated relative to $\hat{f}$ by an angle $\alpha_0$ and shifted by $r_0 = (r_0 \cdot \cos(\eta_0), r_0 \cdot \sin(\eta_0))$. The cross-correlation function

$$c(\alpha, r, \eta)=\int\int\tilde{f}(p,\vec{\xi})\hat{g}(p-r\cdot\sin(\varepsilon+\eta),\varepsilon+\alpha)\,dp\,d\varepsilon \qquad (4)$$

then has its maximum at $(\alpha_0, r_0, \eta_0)$.

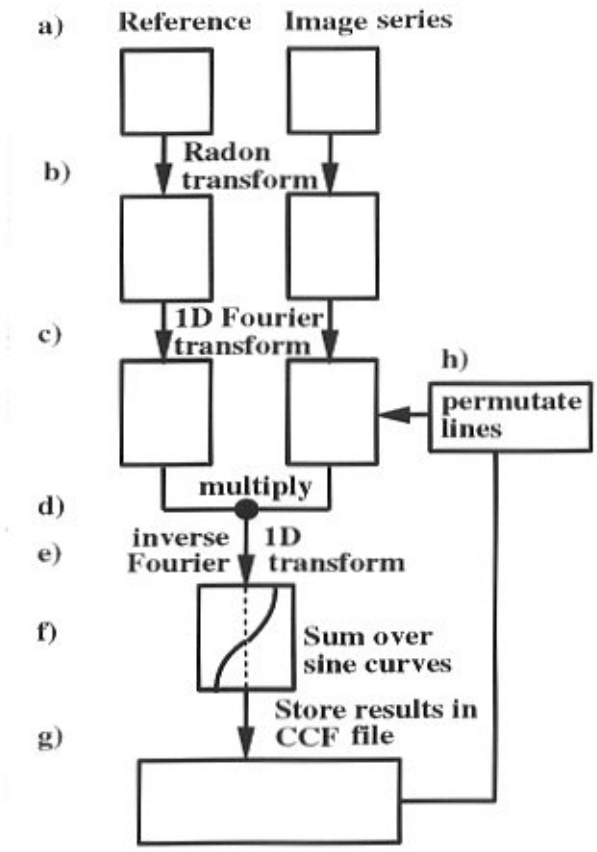


**Figure 1**. Simultaneous translational/rotational alignment of an image series relative to a fixed reference. Both reference and image series (**a**) are Radon transformed (**b**), followed by a one-dimensional Fourier transform (**c**) along p (Eqn. 2). The Fourier Radon transform of the image is multiplied with the Fourier Radon transform of the reference (**d**) followed by a one-dimensional inverse Fourier transform (**e**). A series of cross-correlation coefficients is calculated by summation over sine curves (**f**). Their amplitudes correspond to the size of the shift and their phases to the shift direction. These cross-correlation coefficients are stored in the cross-correlation file (**g**) (see Figure 2). The lines in the Fourier Radon transform of the image are then permutated and the calculations repeated for the next orientation, starting at step (d).

---

The alignment procedure can be directly extended to an alignment of projections relative to a three-dimensional reference. The cross-correlation function then becomes

$$c(\phi, \theta, \alpha, r, \eta)=\int\int\tilde{f}'_{\phi,\theta}(p,\vec{\xi})\hat{g}(p-r\cdot\sin(\varepsilon+\eta),\varepsilon+\alpha)\,dp\,d\varepsilon \qquad (5)$$

$\hat{f}'_{\phi\theta}$ is the cross-section through the three-dimensional

**Table 1**. Comparison of average residual shifts, rotations and resolution limits.

| | Separate translational/rotational alignment | | | | Simultaneous alignment | | | |
|---|---|---|---|---|---|---|---|---|
| | residual | | resolution | | residual | | resolution | |
| | rotation | translation | (DPR) | (FRC) | rotation | translation | (DPR) | (FRC) |
| test 1 | 9.7 | 0.95 | 3.9 nm | 2.3 nm | 1.25 | 0.13 | 2.8 nm | 1.3 nm |
| test 2 | 34.2 | 2.1 | 3.9 nm | 3.7 nm | 1.76 | 0.20 | 3.2 nm | 2.1 nm |

Comparison of average residual shifts (in pixels), rotations (in degrees) and resolution limits of the resulting average images after a traditional rotational/translational alignment versus a simultaneous rotational/translational alignment (DPR: Differential Phase Residual; FRC: Fourier Ring Correlation). Test 1 shows the residuals after several steps of alignment, i.e., centering, dynamic reference alignment followed by fixed reference alignment. Test 2 shows residuals after a single fixed reference alignment.

Radon transform at angles ($\phi$, $\theta$).

For higher computational efficiency the Radon transform of the reference as well as those of all projections are Fourier transformed (Fig. 1). The cross-correlation is calculated by line-by-line multiplication of Fourier-Radon transforms followed by inverse radial Fourier transformation. The integration over $\varepsilon$ is done as a summation across the lines along curves $c(\varepsilon) = r \cdot \sin(\varepsilon+\eta)$.

The rotation of the projections can be applied to their Fourier-Radon transforms by a commutation of lines. Shifts can also be applied to the Fourier-Radon transforms by phase multiplication. If the Radon transform is calculated with an angular increment of $\Delta\phi$, the number of sampling points per line is K, and the shift vector is $r \cdot (\cos(\eta),\sin(\eta))$, then the phase factor P for the Fourier coefficient k in line n is

$$P = \exp[2 \cdot \pi \cdot i \cdot r \cdot \cos((n-1) \cdot \Delta\phi - \eta) \cdot k/K] \qquad (6)$$

Like the traditional rotational and translational alignment algorithm the new algorithm can also be implemented either as alignment algorithm relative to a fixed reference or as an iterative algorithm with a dynamic reference. (*Note*: Originally this method had been called *reference free* alignment [11]). In the latter case one image is chosen as the first reference and the next image is aligned to this reference and added to create a new reference for the following image. Alternatively an average in two dimensions or a three-dimensional Radon transform is created as a first reference from the projection series with randomly assigned angles. Whereas in two dimensions the number of measurements averaged is the same for each point, in the three-dimensional Radon transform this number varies from one line to the next. Here, each radial line in the Radon transform has an averaging index that keeps track of the number of projection lines used for each line in three dimensions.

In three dimensions the alignment with dynamic reference is done in the following way: The lines that form the intersection of the projection through the three-dimensional Radon transform are determined. Each line is multiplied by its averaging index. The corresponding line of the current projection is subtracted, the index reduced by 1, and the result divided by the new averaging index. The orientation and relative position of the Radon transform of the projection is determined according to equation (5) and is averaged back into the three-dimensional Radon transform using the reverse of the procedure for subtraction. Lines that have an averaging index of 0 are skipped in the calculation of the cross-correlation.

For three-dimensional alignment relative to a fixed reference, only the cross-correlation function (eqn. 5) is used.

The alignment procedures that use a dynamic reference are iterated. As stated earlier, for higher computational efficiency each image is Radon transformed, followed by a radial Fourier transform before the alignment. Averaging in two and three dimensions is then done in Fourier space.

The translational alignment is implemented with a fixed accuracy, currently 1 pixel. The shift coordinates are determined in polar coordinates. For a 1 pixel shift, 8 cross-correlation coefficients are calculated for angles $\eta$ (eqn. 2) with values of $0^\circ$, $45^\circ$, $90^\circ$, $135^\circ$, $180^\circ$, $225^\circ$ and $270^\circ$. For a 2 pixels shift the $360^\circ$ angular range is divided into 16 intervals, and for an n-pixel shift into $n \cdot 8$ intervals. Figure 2 shows a cross-correlation function of a two-dimensional simultaneous translational/rotational alignment with a maximum at an angle of $78^\circ$ and a shift of $9 \cdot (\cos 70^\circ, \sin 70^\circ)$.

**Three-dimensional reconstruction**

To observe the progress of the alignment in three dimensions, a fast Two-step Radon Inversion Procedure (TRIP) has been developed. The three-dimensional Radon transform as implemented is sampled on a polar grid. Whereas this sampling scheme uses more points than necessary according to Shannon's sampling theorem, the regular grid simplifies many calculations. The three-dimensional Radon transform is calculated in two steps. In step one, a series of projections forming a single-axis tilt series is calculated from the three-dimensional real space volume. In step two, each projection is then Radon transformed in two dimensions. As a result, each two-dimensional Radon transform then forms a θ-slice (z-direction) in the three-dimensional transform. The radial coordinate increases along the line of each slice (x-direction) and the angle ϕ varies with y. For the inversion an $r^*$-weighted back-projection algorithm has been written. The inversion follows the opposite sequence of the forward Radon transform. First, two-dimensional reconstructions are calculated for each θ-slice, which recreates the "single-axis tilt series". From this series the three-dimensional volume is calculated by a second two-dimensional inversion in slices perpendicular to the y-axis. This procedure is very fast and can take as little as three minutes for a 64x64x64 reconstruction done on a VAX alphastation.

The $r^*$-weighted back-projection can easily be replaced with other two-dimensional inversion algorithms, e.g., a moving window Shannon interpolation [9, 10] or a Fourier Bessel inversion [3].

The reconstruction algorithm can be used independently of the alignment procedure for a reconstruction from random projections. A part of the dynamic reference alignment procedure is averaging of projections into the three-dimensional Radon transform at given angles. Thus a series of projections with known angles can be averaged into a three-dimensional Radon transform, which can then be inverted. Like the averaging algorithm, the inversion algorithm works for real space Radon transforms and for Fourier space Radon transforms.

If the sampling of the three-dimensional Radon transform is complete (i.e., there are no empty lines), the algorithm works essentially with the same accuracy as other algorithms specifically written for arbitrary tilt geometry (discrepancy (e.g., [1, 2]) ~12% for general geometry weighting versus ~8% for the current algorithm). However, when large angular sampling gaps are present, the weighted back-projection for arbitrary geometry works better. The difference in performance can be easily explained. A true three-dimensional reconstruction algorithm is able to interpolate between measurements coming from all directions, whereas the measurements available to the current algorithm either need all be in the same θ-plane (in step 1) or all in the same y-z-plane (step 2).

The reconstruction algorithm is an averaging method in three dimensions. Thus, a number of the same error measures can be calculated as in other averaging procedures. Among them are a determination of the standard deviation of every point in the three-dimensional Radon transform, which when inverted leads to an error estimate for every pixel in the three-dimensional reconstruction. Because the averaging step can be done in real or in Fourier space, calculations like three-dimensional Q-factors [8, 19] and spectral signal to noise ratios [17] are possible.

## Test Calculations and Applications

**Alignment in two dimensions**

Simultaneous translational and rotational alignment has been applied to a series of 448 images of the 50S ribosomal subunit prepared in vitreous ice.

The new simultaneous alignment algorithm and the traditional separate translational/rotational alignment methods were compared in two series of test calculations. The first test (test 1 in Table 1) consisted of three steps:

First, all images were centered, as is traditionally done, by cross-correlation to the image of a low-pass filtered disk with the approximate size of the particle [13]. Second, a dynamic reference alignment was done, followed in the third step by a fixed-reference alignment. The reference used was the average that was obtained in the previous step. Residual shifts and translations were then determined by another fixed reference alignment.

In a second test (test 2 in Table 1) both alignment procedures were applied directly to the non-centered original images using a fixed reference. This was again followed by a second alignment step to determine residual shifts and rotations.

In test 1 the residual shifts turned out to be approximately the same, less than 1 pixel. One pixel was the accuracy to which the simultaneous alignment determined the translation. The differences are larger for the rotational alignment, where the simultaneous alignment was more accurate. As expected, the difference in performance of the two algorithms is much larger in test 2, where the simultaneous alignment produces average residual shifts and rotations that are smaller by a factor of about 20. There are two advantages to the simultaneous alignment algorithm. One advantage is a simple time factor: an alignment with the new algorithm takes approximately the same amount of time as a single iteration of the non-simultaneous alignment algorithm. The faster performance results from not needing multiple iterations. A second advantage is that the simultaneous alignment algorithm when applied to a fixed reference will find the best global maximum in the rotational/translational cross-correlation function, whereas the traditional algorithm is more prone to finding a local

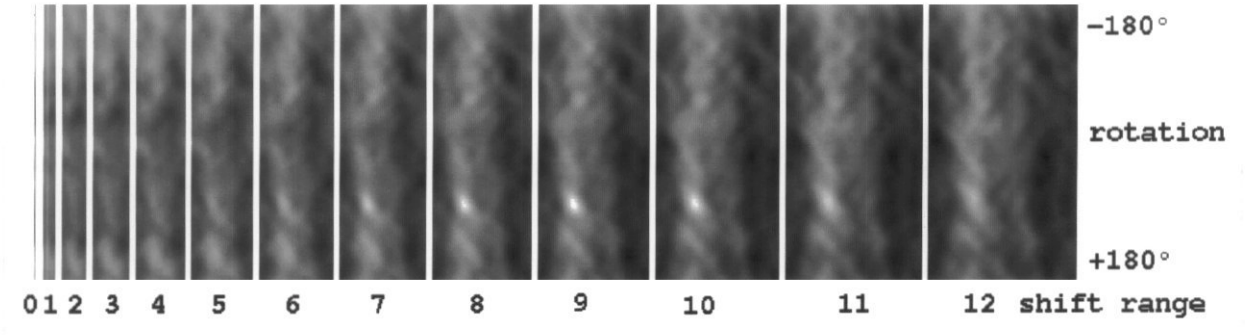


**Figure 2**. Cross-correlation function from a two-dimensional simultaneous translational/rotational alignment. The function shows bands of increasing width. The width of each band corresponds to the number of directions searched for each value r. In each band the horizontal axis is the direction of the shift vector, and the vertical axis is the rotation of the image.

maximum.

**Three-dimensional alignment and reconstruction**

As a test object a volume was created containing eleven spheres in random positions (Fig. 3). Two hundred projections were calculated from this volume with random angles. A different set of random angles was assigned to these projections and a reconstruction was calculated that essentially, because of the arbitrary angle assignment, showed no significant features. The three-dimensional alignment procedure with dynamic reference was then applied. In sequence each projection was subtracted from the volume, the cross-correlation function (Eqn. 5) was calculated, and the projection was averaged back into the volume with the angles found. Figures 4, 5 and 6 show the results of this calculation. Features already appear after the first iteration and the pattern of spheres appears after iteration 7. TRIP was used in the calculation of all reconstructions shown.

This example uses a noise-free data set, and it is clear that the three-dimensional dynamic reference alignment algorithm will not perform as well with real data. The signal-to-noise ratio of Radon transforms of images of frozen hydrated samples is on the order of 0.3, and trials with raw data thus far have not yielded convincing results. The current implementation can still be improved to make better use of the information present, and the noise limit of the algorithm will be determined once these improvements have been implemented. It has been shown earlier [14], however, that the alignment algorithm works for a fixed-reference alignment down to a signal to noise ratio of less than 1. The dynamic reference alignment algorithm is the first

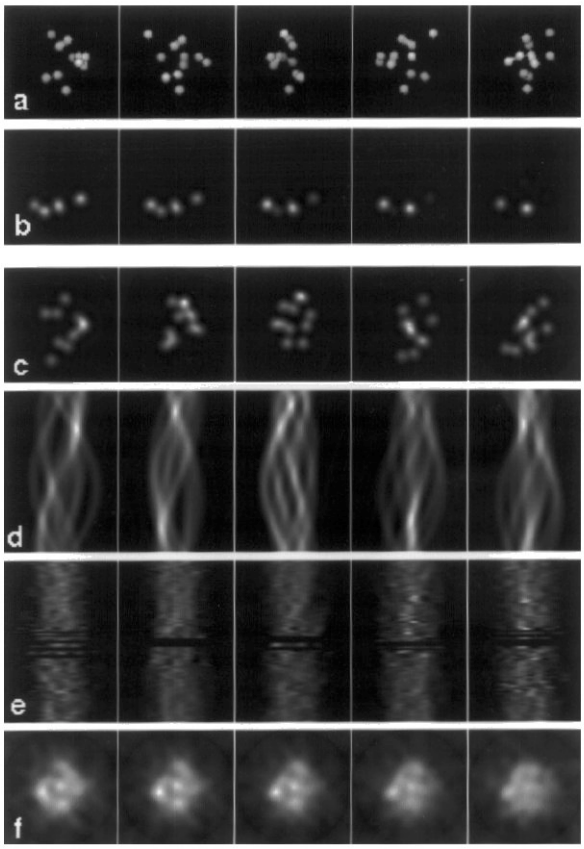


**Figure 3**. Test of three-dimensional dynamic reference alignment. (**a**) Surface representations of the model volume, (**b**) Slices through the volume, perpendicular to z near the center, (**c**) Projections of the volume, (**d**) Selected cross-sections through the three-dimensional Radon transform. The angles correspond to the angles of the projections shown in (c), (**e**) Sections through the three-dimensional Radon transform that was created from the projections with arbitrarily assigned angles. Slices correspond to the same θ-angles as the cross-sections shown in (d); (**f**) Slices through the reconstruction calculated from (e). The surface representation of this volume is shown in Figure 4, panel 0.

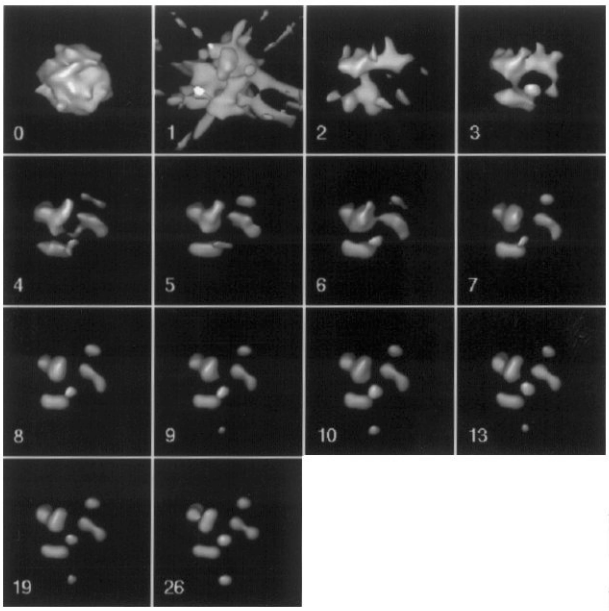


**Figure 4**. Surface views of the volume during iteration of the dynamic reference alignment in three dimensions. Numbers indicate iteration. Iteration 0 is the start volume created from projections with arbitrarily assigned angles.

implementation of the extension of this original algorithm as it was proposed in [14].

## Conclusion

Radon transform-based methods have been presented that allow a reconstruction from random projections and provide a technique for simultaneous translational and rotational alignment in two and three dimensions. The simultaneous alignment worked faster and with substantially higher accuracy than traditional methods that alternate between translational and rotational alignments. Fixed-reference and dynamic-reference alignment procedures have been developed for two and three dimensions. They have been combined with a fast Radon inversion algorithm. By itself, this algorithm can also be used for three-dimensional reconstruction from projections with any set of known orientations. The first step in building the three-dimensional Radon transform is an averaging procedure that averages all lines that are common to more than one projection. The fact that the three-dimensional Radon transform is built up by averaging allows for the calculation of error measures and resolution criteria that to date have mainly been used in two-dimensional alignment methods. The averaging can either be done by averaging Fourier Radon transforms, which should allow the calculation of Q-factors, or by averaging real-space

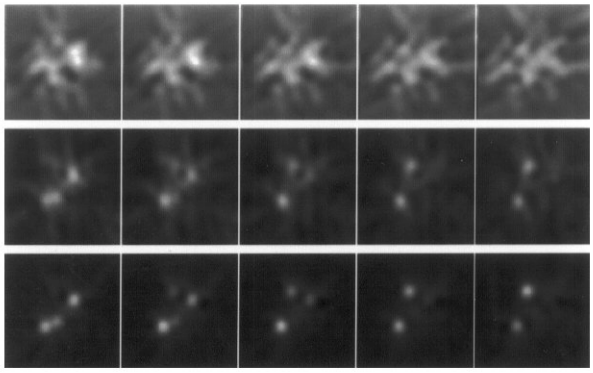

**Figure 5**. Sections through the reconstruction after 1, 13 and 26 iterations.

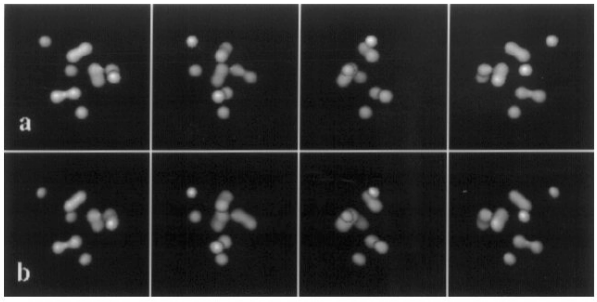


**Figure 6**. Comparison of original volume (**a**) and reconstructed volume (**b**) using the dynamic reference alignment method in three dimensions.

Radon transforms which allows for the calculation of real-space variance measures.

## Acknowledgements

This work was supported by grants from NSF (BIR 9115534 and DBI9515518) and NIH (RO1 GM29169, 5RO1 AR40615, and P41 RR01219).

## References

1. Colsher JG (1976) Iterative three-dimensional image reconstruction from projections: Applications in electron microscopy. Doctoral Thesis, Lawrence Livermore Laboratory, University of California, Livermore.

2. Colsher JG (1977) Iterative three-dimensional image reconstruction from tomographic projections. Comp Graph Image Proc **6**: 513-537.

3. Crowther RA, DeRosier DJ, Klug A (1970) The reconstruction of a three-dimensional structure from projections and its application to electron microscopy. Proc

Roy Soc Lond A **317**: 319-340.

4. Deans SR (1983) The Radon Transform and Some of its Applications. John Wiley & Sons, New York.

5. Farrow NA, Ottensmeyer FP (1992) A posteriori determination of relative projection directions of arbitrary oriented macromolecules. J Opt Soc Am A **9**: 1749-1760.

6. Goncharov AB, Vainshtein BK, Ryskin AI, Vagin AA (1987) Three-dimensional reconstruction of arbitrary oriented identical particles from their electron photomicrographs. Sov Phys Crystallogr **32**: 504-509.

7. Guckenberger R (1982) Determination of a common origin in the micrographs of tilt series in three-dimensional electron microscopy. Ultramicroscopy **9**: 167-178.

8. Kessel M, Radermacher M, Frank J (1985) The structure of the stalk surface layer of a brine pond microorganism: Correlation averaging applied to a double layered lattice structure. J Microsc **139**: 63-74.

9. Lanzavecchia S, Bellon PL (1993) A bevy of novel interpolating kernels for Shannon reconstruction of high band pass images. Universita degli Studi di Milano, Quaderni del Dipartimento di Mathematica 54.

10. Lanzavecchia S, Bellon PL, Scatturin V (1993) SPARK, a kernel of software programs for spatial reconstruction in electron microscopy. J Microsc **171**: 225-266.

11. Penczek P, Radermacher M, Frank J (1992) Three-dimensional reconstruction of single particles embedded in ice. Ultramicroscopy **40**: 33-53.

12. Pintsov DA (1988) Invariant pattern recognition, symmetry and Radon transforms. J Opt Soc Am A **6**: 1544-1554.

13. Radermacher M (1988) Three-dimensional reconstruction of single particles from random and nonrandom tilt series. J Electr Microsc Techn **9**: 359-394.

14. Radermacher M (1994) Three-dimensional reconstruction from random projections: orientational alignment via Radon transforms. Ultramicroscopy **53**: 121-136.

15. Radermacher M, Wagenknecht T, Verschoor A, Frank J (1986) A new 3-D reconstruction scheme applied to the 50S ribosomal subunit of *E. coli*. J Microsc **141**, RP1-RP2.

16. Radon J (1917) Über die Bestimmung von Funktionen durch ihre Integralwerte längs gewisser Mannigfaltigkeiten (On the determination of functions from their integral values along certain manifolds). Ber Verh der Königlich Sächsischen Ges Wiss Leipzig, Math Phys Klasse **69**: 262-277.

17. Unser M, Trus BL, Steven AC (1987) A new resolution criterion based on spectral signal to noise ratios. Ultramicroscopy **23**: 39-52.

18. Van Heel M (1987) Angular reconstitution: a posteriori assignment of projection directions for 3D reconstruction. Ultramicroscopy **21**: 111-124.

19. Van Heel M, Hollenberg J (1980) The stretching of distorted images of two-dimensional crystals. In: Electron Microscopy at Molecular Dimensions. Baumeister W (ed). Springer Verlag, Berlin/New York. pp 256-260.

## Discussion with Reviewers

**G. Harauz**: To what extent has it proven possible, in the author's experience, to "mix" reconstructions from negatively-stained SECReT preparations and from frozen-hydrated randomly oriented ones?

**Author**: I have not "mixed" data from negatively stained specimens and frozen hydrated specimens. In my opinion it may be possible to use the envelope information obtained from a negatively stained specimen as a reference for alignment of frozen hydrated data. However, negatively stained and dried specimens can be severely flattened, which will show in a reconstruction from random conical data. Only if a reasonable assumption can be made on how to correct for this flattening may a valid reference for alignment be created. These effects can be severe as shown e.g., in [20]. The flattening here is associated with a twisting of the upper part of the molecule.

## Additional Reference

20. Radermacher M, Rao V, Grassucci R, Frank J, Timerman AP, Fleischer S, Wagenknecht T (1994) Cryo-electron microscopy and three-dimensional reconstruction of the calcium release channel/ryanodine receptor from skeletal muscle. J Cell Biol **127**: 411-423.